Low Temperature Physics/Fizika Nizkikh Temperatur, 2014, v. 40, No. 8, pp. 946–958

Review of modern instrumentation for magnetic measurements at high pressure and low temperature

X. Wang and K.V. Kamenev

School of Engineering and Centre for Science at Extreme Conditions, University of Edinburgh, Edinburgh EH9 3JZ, United Kingdom
E-mail: k.kamenev@ed.ac.uk

Received March 4, 2014, published online June 23, 2014

High-pressure magnetic susceptibility experiments can provide insights into the changes in magnetic behavior and electric properties which can accompany extreme compressions of material. Instrumentation plays an important role in the experimental work in this field since 1990s. Here we present a comprehensive review of the high-pressure instrumentation development for magnetic measurement from the engineering perspective in the last 20 years. Suitable nonmagnetic materials for high pressure cell are introduced initially. Then we focus on the existing cells developed for magnetic property measurement system (MPMS®) SQUID magnetometer from Quantum Design (USA). Two categories of high pressure cells for this system are discussed in detail respectively. Some high pressure cells with built-in magnetic measurement system are also reviewed.

PACS: **07.35.+k** High-pressure apparatus; shock tubes; diamond anvil cells;
07.55.–w Magnetic instruments and components;
62.50.–p High-pressure effects in solids and liquids;
74.62.Fj Effects of pressure;
75.40.–s Critical-point effects, specific heats, short-range order.

Keywords: high pressure, magnetization and magnetic susceptibility measurement, piston-cylinder cell, opposed-anvil cell, SQUID magnetometer.

1. Introduction

Magnetization (M) is a fundamental physical property characterizing the response of a material to applied magnetic field. The dependence of temperature (T), field (H), and pressure (P) could be used to investigate the nature of magnetic interactions, the value of the exchange parameters, the critical T, H, and P of magnetic phase transitions, etc. A.A. Galkin has been one of the pioneers of magnetic properties measurements at high pressure. Using a piston-cylinder cell with a built-in solenoid for generating high pulsed magnetic fields, the group led by him mapped and investigated the P–T-phase diagram of MnAs [1].

As the modern magnetometer can provide precise control in temperature and magnetic field change, high pressure instrumentation for the magnetometer became an important field of magnetization study in past two decades. The magnetic property measurement system (MPMS®) manufactured by Quantum Design (USA) [2] is the most popular commercial magnetometer as the sensitivity of this magnetometer reaches 10^{-8} emu over a wide range of temperature and magnetic fields. As the excellent sensitivity of this instrument is based on the integrated superconducting quantum interference device (SQUID), it is usually been referred as SQUID magnetometer.

This review mainly covers existing high pressure cells for the MPMS SQUID magnetometer from 1996 to date. Design constrains and suitable materials for building the cell are discussed first. Then two types of high pressure cells for the SQUID magnetometer, cylinder and opposed anvils are described separately. The other high pressure cells for magnetic measurement with built-in coils are discussed last.

2. dc and ac measurement

Most of magnetic measurements are performed by dc and ac techniques which are two entirely different ways to investigate magnetic properties. Both these techniques rely on detection coils used to measure the variation in the magnetic flux from the magnetized sample. The fundamental difference between these two techniques is how to create the flux variation. In a dc magnetization measurement, a sample is subjected to and magnetized by a constant dc

© X. Wang and K.V. Kamenev, 2014

magnetic field generated by an iron core or superconducting solenoid (such as the SQUID magnetometer) then move relative to a detection coil. The variation in the magnetic flux density induces a current in the detection coil based on the movement of the magnetized sample. The induced current in the detection coil can be measured and related to the material magnetization. In contrast, in ac measurement, the sample is centered within a driving coil while driven with an external alternative (ac) magnetic field. This allows the time-dependent magnetization to be measured in a second detection coil without sample motion. Even though the commercial SQUID magnetometer provides both measurement techniques, most high-pressure magnetic measurements in SQUID were performed in dc mode as the cell material issue. ac techniques were used more widely in high pressure cells with built-in coils which are presented in Sec. 7.

3. Design challenge of high pressure cells for SQUID magnetometer

The size limitation is the first challenge for designing a high pressure cell for MPMS as the diameter of sample chamber in MPMS is only 9 mm diameter, which means external diameter of the cell must smaller than 9 mm to be fit in. Therefore, the published cell designs were usually described as “miniature” due to the dimensions of such cells are much smaller than conventional high pressure apparatus. Material selection is another important consideration in design. Magnetic measurements normally involve high magnetic field and low temperature. The material used in construction high pressure cell needed to be carefully considered in such extreme environment.

There are three fundamental requirements for material. First, the material strength needs to be high enough to withstand high pressure. Second, the magnetization of the material is desired to be small and insensitive to the applied magnetic fields, the sensitivity of the cell can be increased if it was made of lower background material. Last, the mechanical and magnetic property of the material is desired to be stable for a broad temperature particular in extremely low temperature. Apart from 3 constrains above, sometimes other factors will matter such as commercial availability and price. There are a few suitable materials from the existing publication so far. None of these materials listed here is absolute perfect, the instrument scientists need to find their own balance among these considerations such as high pressure range, high sensitivity, budget, material availability, etc.

Figures 1 and 2 show the magnetic susceptibility of three candidate materials for the magnetic cell. BeCu alloy is the most popular material for pressure cells in the magnetization measurement at present. The magnetic susceptibility is low as Be and Cu are both diamagnetic element. The ultimate tensile strength can achieve 1.4 GPa after fully hardening at

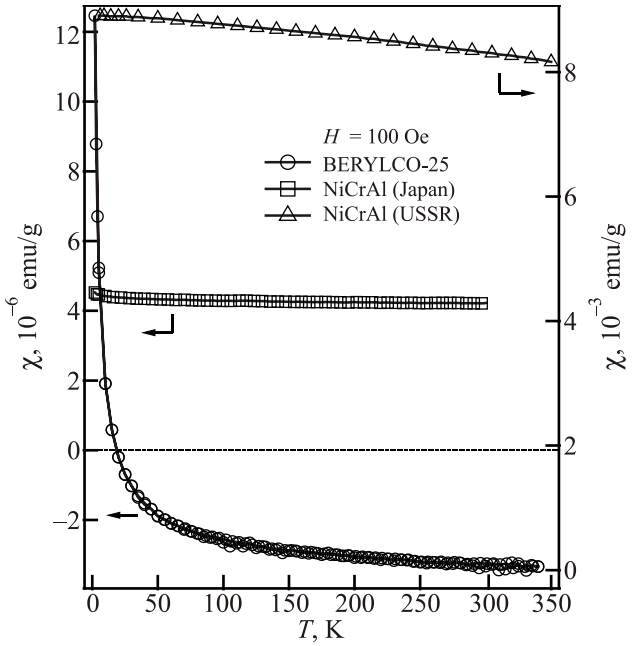

Fig. 1. Temperature dependence of the magnetic susceptibility of BeCu alloy (BERYLCO-25) from NGK [3], and NiCrAl alloy from Japan [9] and the USSR region [8]. The BERYLCO-25 is with 0.2% Co and 0.6% Ni+Fe impurity. The arrows indicate which scale the data is associated with. The susceptibility was measured in 100 Oe field over the temperature range from 300 to 2 K. It is clear that the NiCrAl from Japan is much lower than the one from former USSR region.

315 °C for 2 hours [3]. It is commercially available as standard rod or sheet in the market which is convenient and economical to purchase. As shown in Fig. 1, the magnetic susceptibility of BeCu increases noticeably at low temperature due to impurity containment of nickel or cobalt. The commercial BeCu alloy normally contains Ni and Co with the rates of 0.2–0.5% to avoid the toxic beryllium oxide appears on the alloy surface [4]. The magnetization of BeCu depends

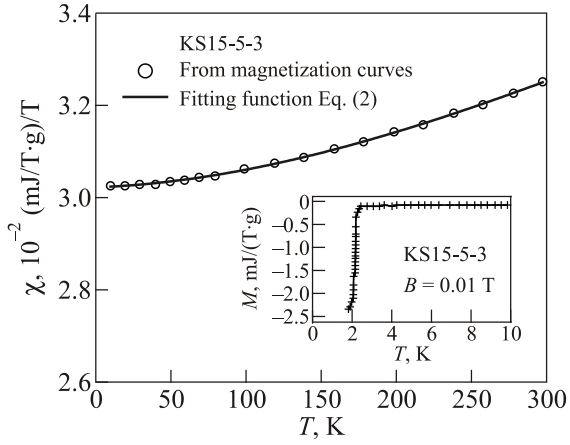

Fig. 2. The magnetization of KS15-5-3 for several temperature, the inset shows the temperature dependence of the magnetization at B = 0.01 T, superconducting phase transition occurs at 2.5 K. Figure reprinted with permission [4].

on the added impurity of Co and Ni and the amount. Ni is preferred to Co as its magnetic moment is smaller [5–7]. Apart from that, the mechanical properties of BeCu are very stable at low temperature, the plasticity even increase [8]. This is a unique advantage for constructing low temperature cell as it would be safer without brittle failure.

NiCrAl is a promising alloy for high pressure cell due to the nonmagnetic and high strength characteristic. The heat treated alloy is with tensile strength 2.2 GPa [9]. However, the main issue of this alloy is the availability. It is called Russian alloy as it was only available in former USSR region with small quantity [10]. It was not commercially available until successfully reproduction in Japan on 2002 [9], the magnetic background of the alloy was improved significantly as shown in Fig. 1. There is another nonmagnetic alloy Co–Ni–Cr–Mo (MP35N) which had been used to fabric piston-cylinder high pressure cells [10]. The yield strength of MP35N is 1.79 GPa. However, the magnetic susceptibility of MP35N alloy is much higher than other nonmagnetic alloy [9], which made it less favorable in construction a cell for SQUID magnetometer.

High purity CuTi alloy with 3 wt% was reported with extremely lowest magnetic susceptibility among the high pressure alloys so far [7]. The susceptibility of diamagnetic copper component and paramagnetic component titanium almost cancel out in the alloy. The susceptibility of this alloy is reported with $3\cdot10^{-9}$ emu/g at room temperature, $8\cdot10^{-8}$ emu/g at 1.8 K [4]. The susceptibility of this alloy increase at low temperature was caused by the impurity. The tensile strength is between 680–1000 MPa [4]. Again, availability issue is the main disadvantage as the alloy is not a widely commercialized alloy as BeCu. The high strength and high purity CuTi seems only available in Japan so far.

A β phase titanium alloy KS15-5-5-3 reported by Kamishima and co-workers [4] is a good candidate material because this alloy is extremely pure without ferromagnetic component. The magnetic susceptibility is closed to $3.03\cdot10^{-2}$ (mJ/T·g)/T at 3 K and almost featureless (Fig. 2) at broad temperature range. For convenience, the magnetic unit is converted to the "emu/g" then the number is $3.03\cdot10^{-6}$ emu/g. The tensile strength is 1.76 GPa after mechanical rolling and heat treatment, which is higher than harden BeCu alloy. The only problem is that the material experienced a superconducting phase transition at 2.5 K when external magnetic field applied. Therefore, this alloy is not usable for magnetic measurement below 2.5 K. In addition, one common shortcoming of titanium alloy is that the alloys tend to be brittle at low temperature, which is why the titanium alloy is not popular in cryogenic instrument.

Recently, high-strength engineering plastic material start to be used for building high pressure cells [11]. Engineering plastic is a valuable potential material for high pressure engineering in magnetic measurement. Particular in diamond anvil cell which does not require much load to applied high pressure on tiny sample. Section 6 shows the recent progress in constructing a DAC from engineering plastic which enable the high pressure ac susceptibility measurement can be measured in the commercial SQUID magnetometer directly.

4. Pressure calibration in high pressure cells in magnetization study

There are several ways to calibrate pressure in high pressure cells. As the superconducting transition temperature T_c of Pb, Sn and In had been calibrated with pressure [12], these metals are widely used as manometer in high pressure study at low temperature because of the accuracy. For piston-cylinder cells, pressure in the cell can be estimated indirectly by measuring the overall length extension or radial expansion of the cell at room temperature. For diamond anvil cell, ruby fluorescence method [13] is another way to measure the pressure directly at room temperature. For high pressure study at low temperature, the pressure measured at room temperature usually needs to be calibrated with Pb manometer if pressure change cannot be neglected in the study. Particular for piston-cylinder cell, pressure change can be up to 0.4 GPa when temperature was cool down to 5 K (Fig. 3). The thermal expansion coefficients difference in the cell materials, pressure transmitting medium and the sample itself are considered as the main contribution to the pressure variation during cooling or heating. Furthermore, the pressure transmitting fluid might changes its state from liquid to solid at low temperature which would induced pressure change as well. Manganin pressure sensor had been found the most accurate way to measure the pressure in piston-cylinder cell, but this method is only limited to this type of cell. The temperature induced pressure variations in piston-cylinder had been studied extensively [14,15]. Figure 3 shows the pressure change of three commonly used pressure transmitting medium.

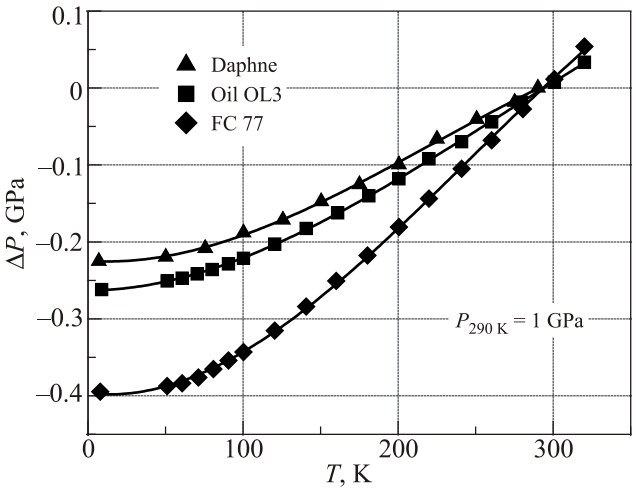

Fig. 3. Temperature induced pressure variation in clamped cell reported by Kamarád *et al.* [14].

5. Cylinder type high pressure cells for MPMS SQUID magnetometer

Early pressure cells for SQUID magnetometer were built as cylinder type. This type of pressure cell is very simply to fabricate and with large sample volume. Most of cells were with pressure limit no higher than 1.2 GPa. The first high pressure cell made for the MPMS SQUID magnetometer was reported by Reich and Godin [16] in 1996. The cell is made of titanium alloy (Ti-6Al-6V-2Sn) and only simply consists of two parts, a single cylinder cell body and a closed nut (see Fig. 4). It is named miniature cell as the overall diameter is 7.7 mm and overall length is only 41 mm. The maximum pressure was reported about 0.4 GPa by solidifying the pressure medium liquid gallium at liquid nitrogen temperature. This cell had been used to investigate the influence of the pressure on ceramic superconductors $HgBa_2Ca_2Cu_3O_{8+x}$ (1223) compound. The superconducting temperature of this material was found increased from 133 K at ambient pressure to 136 K at 0.4 GPa pressure. As the pressure generation of this cell is uncontrollable by this setting, piston-cylinder cell are more commonly used in following designs.

Figure 5(a) shows a typical piston-cylinder high pressure cell developed in 1996 for SQUID by Diederichs *et al.* [17]. The pressure of this cell is created by applying the load in a hydraulic press. In the meantime, the thread on the piston end is used to lock the pressure by tightening the hollow retaining screw. The cell can be removed from the press and insert into the SQUID after pressurization. The body of the cell is a long cylinder made of BeCu alloy and the cell was reported with 1 GPa pressure capability. The sample immersed with fluorinert FC75 pressure transmit medium and pressed directly by a pair of quartz spacers which keeps the sample away from the ends of the cell yielding a more symmetric distribution of the background signal. Sealing mechanism of this cell was not mention in the paper. The pressure was found able to be calibrated by

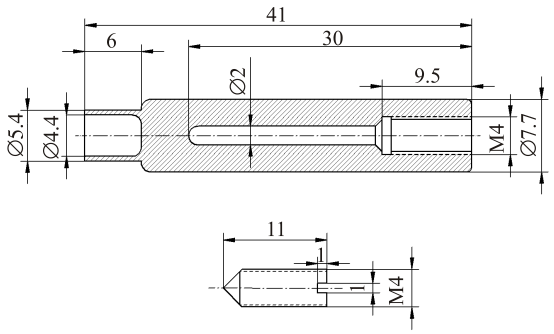

Fig. 4. The design of the pressure cell reported by Reich and Gordin [16]. Sample and a Pb manometer was loaded into the cell and immersed in the liquid gallium pressure medium, the dimensions are in mm. Figure reprinted with permission [16].

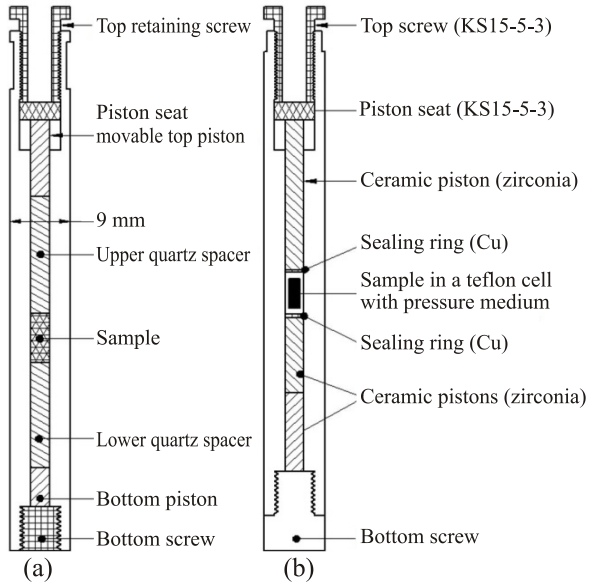

Fig. 5. Schematic of the cell reported by (a) Diederich *et al.* [17] which is made of BeCu, overall length is 210 mm, and (b) Kamishi *et al.* [4], made of KS15-5-3, overall length 120 mm (redrawn, not to scale).

measuring the extension of the overall length of the cell through an optical micrometer at room temperature. Combining with the T_c measurement of a Pb manometer, the pressure and the extension of the cell body is liner related as 42.2 μm/GPa, which enables the pressure can be approximated at room temperature through measuring the extension of the cell body only. The cell was used to measure the magnetic susceptibility of Rb_3C_{60} sample under pressure in the SQUID. The magnetic susceptibility of this material was found decrease under pressure both at 50 K and room temperature.

As showed in Fig. 5(b), an improved design was reported in 2000 [4]. The cell was made of titanium alloy (KS15-5-3) which shows desirable temperature-independent magnetization curve above 2.5 K. This alloy is with lower magnetization and higher material strength in comparison to BeCu alloy. The ceramic (zirconia) piston is with lower magnetic background if compare to quartz piston used in the earlier design [17]. Therefore the sensitivity of this cell is increased by these measures. PTFE capsule was used to contain sample and liquid pressure medium. Cu rings were used for extra seals to prevent leakage and extrusion. The pressure range of this cell is 1 GPa and Sn manometer is used for pressure calibration. The cell had been used in measuring the pressure effect on the one-dimensional antiferromagnet Ni(333-tet) $(\mu\text{-}NO_2)\times(ClO_4)$ which with small magnetization. The main shortcoming of this cell is that it is unable to use at temperature below 2.5 K which is the superconductivity temperature of the titanium alloy in used.

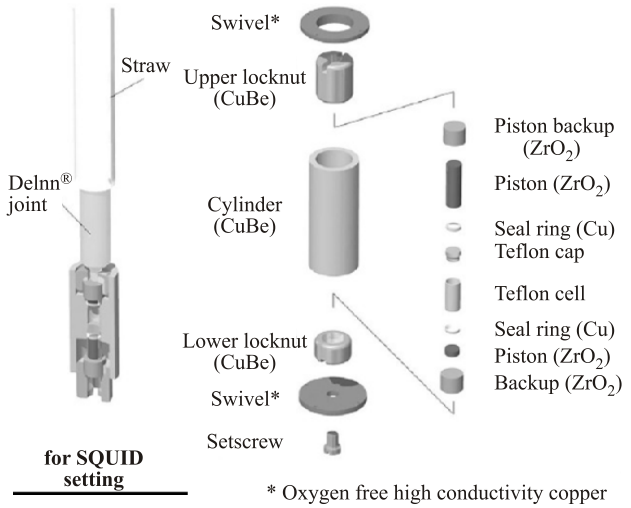

Fig. 6. Schematic drawings of micro high pressure cell [19,20]. Figure reprinted with permission [20].

A similar BeCu version piston-cylinder cell for MPMS SQUID was commercial available from easyLab since 2004, the working principle of the cell is the same with cells reviewed above but pressure capability was increased to 1.2 GPa [18]. Researchers can purchase this type of pressure cell commercially rather than building a similar cell in-house.

A series of short version of piston-cylinder cells were reported by Umehara *et al.* [19] in 2004 and Uwatoko *et al.* [20] in 2005 (Fig. 6). These cells were designed for magnetic and specific heat measurement in on the CeAg sample by a SQUID magnetometer and a standard adiabatic method. These cells were named as micro high pressure cell due to the length of the cell was minimized to 21 mm which is the smallest piston-cylinder cell so far. These cell were made of harden BeCu and maximum pressure was achieve 2 GPa in one cell with 2.5 mm diameter bore. Sn manometer was used for pressure calibration in these cells.

Figure 7 shows the schematic drawing of a different piston cylinder cell reported by Kamarád *et al.* in 2004 [14]. The cell was made of BeCu alloy with 2.5 mm internal diameter and 8.6 mm external diameter with pressure limit up to 1.2 GPa. Hydraulic press was not needed in this design as pressure is generated by tightening the clamp screws. The sample and pressure medium can be loaded directly into the cell without capsule as the Bridgeman mushroom seals are able to seal the moving piston at high pressure, which exclude the magnetic background from the PTFE capsule. Lamé equations were found can be used to approximate the pressure inside cylinder body at room temperature by measuring the radial expansion of the cell body and calibrated the Pb manometer. The cell had been used to study the temperature induced pressure changes from 350 down to 5 K using different pressure transmitting media (Fig. 3).

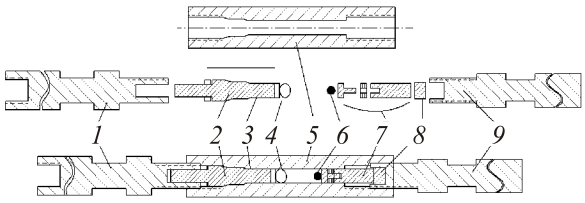

Fig. 7. Schematic drawing of high pressure cell for MPMS designed by Kamarád and co-workers [14]. The cell is with 2.5 mm bore and outer diameter 8.6 mm; (*1*) upper clamping bolt, (*2*) plug, (*3*) seals, (*4*) sample on holder, (*5*) cell body, (*6*) Pb manometer, (*7*) piston with Bridgeman mushroom-type seal, (*8*) piston backup, (*9*) lower clamping bolt.

Kamenev *et al.* [21] reported a long symmetric high pressure cell (Fig. 8) for high-pressure magnetic measurements on a molecular antiferromagnet sample $[N(C_2H_5)_4][FeCl_4]$ up to 1 GPa. The cell body is made of BeCu and the pre-

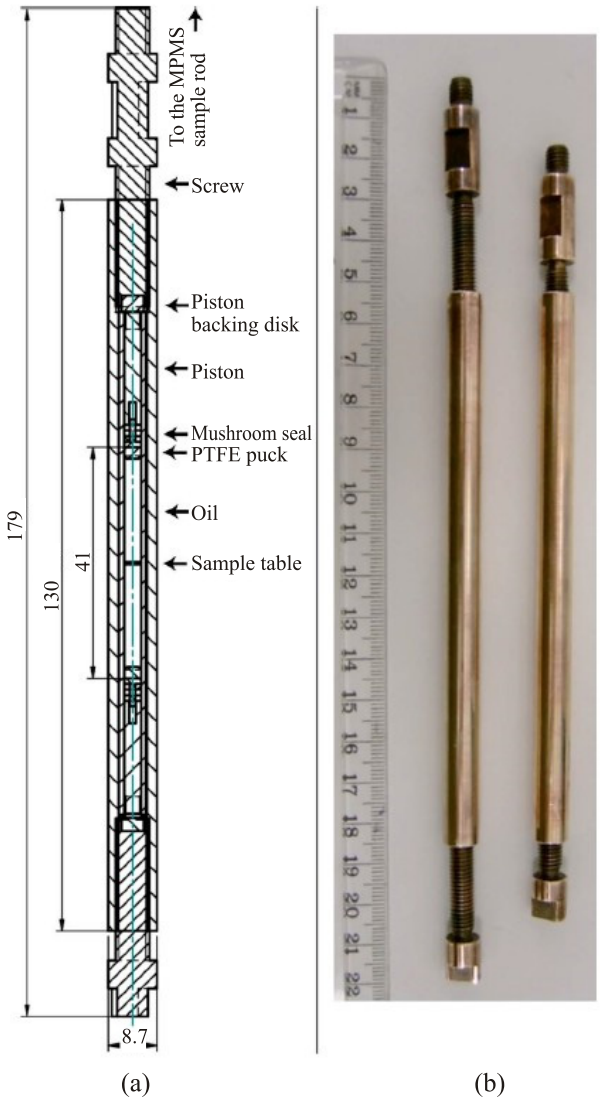

Fig. 8. (a) Drawing of the cell with the distance between the pistons shown for the top applied pressure and (b) photograph of the high pressure cell at ambient pressure (left) and top pressure (right). Figures from Kamenev *et al.* [21].

stressed technique double layer with interference fit was used in constructing the cell to improve the stress distribution compared to the conventional single cylinder cell body. The working principle of this cell is similar to the previous design reported by Kamarád *et al.* [14]. Pressure is generated by tightening the clamp screws but the sample volume is greater as the cell is much longer. The fully symmetry layout of the cell was turned to be very beneficial on background correction and improve the sensitivity of the measurement, which allows sample with low magnetic susceptibility to be measure under high pressure. As the sample has a transition into an antiferromagnetic (AF) phase at T_N = 3.0 K, which is lower than the temperature of the superconductive transition in pressure standards manometer Pb (T_c = 7.20 K), Sn (T_c = 3.20 K), or In (T_c = = 3.40 K). The manometer will create significant background when in superconductive state and screens the sample signal. Therefore, Lamé equations were used to estimate the pressure at room temperature. This pressure measurement needs to be calibrated with measured result of temperature T_c of the superconducting transition in Pb in advance because pressure inside the cell drops at low temperature due to the difference in thermal expansion coefficients of the BeCu alloy and the pressure transmitting fluid used (Daphne oil).

NdRhSn single crystal was found with huge anisotropy of magnetic interactions, Kamarád *et al.* [22] had designed two miniature uniaxial pressure cells for magnetic and neutron-diffraction studies of this crystal in a SQUID magnetometer and in a neutron diffractometer respectively. The schematic drawing of the uniaxial pressure cell for SQUID magnetometer is showed in Fig. 9. The oriented sample is closed by two ZrO-ceramic anvils. The uniaxial force applied on the sample is produced from a set of CuBe Bellville springs. Each set of the springs is inserted into a thin-wall tube and fixed to the cell-squeezing screw. This spring's system was calibrated by compressing it using a precision load transducer in advance. Users can determine the actual force acting in the cell directly from the calibration curve and a measured elastic compression of the springs system inside the cell when tightening the squeezing screw.

In 2008, Sanchez-Benitez *et al.* [15] reported a piston-cylinder cell with a plug for *in situ* pressure measurements

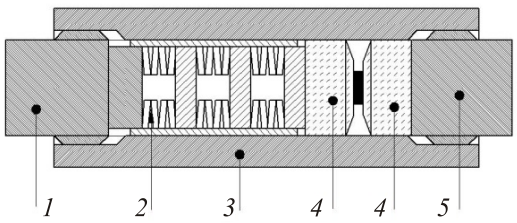

Fig. 9. Schematic drawing of uniaxial pressure cell for MPMS designed by Kamarád *et al.* [22]. (*1*) CuBe squeezing screw, (*2*) set of the Belleville springs, (*3*) cell body, (*4*) ZrO anvils, (*5*) CuBe fixing screw (redrawn, not to scale).

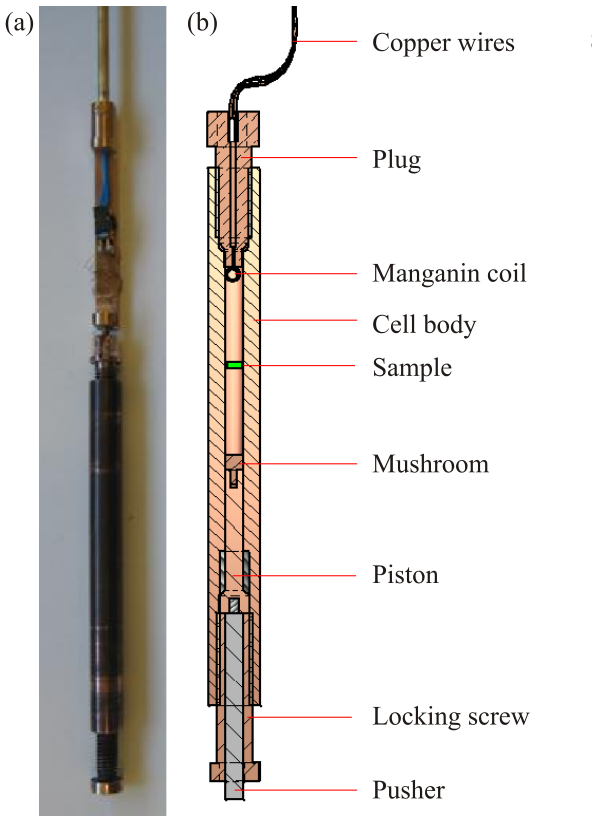

Fig. 10. (a) Assembled pressure cell attached to the MPMS sample rod through and adapter with a 4-pin socket mounted on it. (b) Cross-sectional view of the assembled pressure cell. Figures from Sanchez-Benitez *et al.* [15].

with feed-through wires connected to a manganin pressure sensor which has a known pressure dependence of electrical resistivity (Fig. 10). It provided a mean to monitor pressure continuously during magnetization measurements in MPMS. The true pressure can always be established in the range of temperature in this cell.

Lately, we have built a gas pressure cell to perform a high-pressure study on a spin-crossover nanoparticles (SCONPs) material reported by Titos-Padilla *et al.* [23]. The material exhibits an abrupt transition with large thermal hysteresis centered to room temperature. We found that the hysteresis loop of this material is extremely sensitive up to 100 MPa. Previous piston-cylinder cells are unable to provide pressure control in this small scale. Pressure control by gas cylinder or gas compressor is much more precise and suitable. The cross-sectional view of the gas pressure cell with its key dimensions is presented in Fig. 11(a). It consists of two main components — a cylindrical body and a plug — both of which are made of hardened BERYLCO-25 alloy (tensile strength ~ 1.4 GPa). The cell is connected to an external gas cylinder by means of a steel capillary (Fig. 11(b)). The sample is contained in a PTFE capsule. The outer and inner diameters of the pressure cell were optimized to provide space for a large quantity of sample

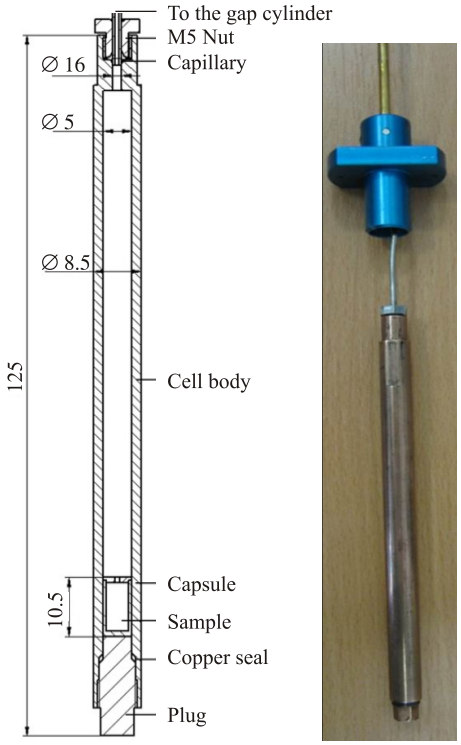

Fig. 11. (a) Drawing of the cell with key dimensions; (b) picture of the assembled pressure cell (unpublished).

and to withstand pressures of up to 100 MPa with the safety factor of 4. Helium gas was used as a pressure-transmitting medium. Pressure was controlled by using a pressure regulator on the gas cylinder.

6. Opposed anvil cells for MPMS SQUID magnetometer

Because of the strength limitation of the nonmagnetic materials, higher pressure range (greater than 2 GPa) requires the use of opposed anvil cells, such as diamond anvil and sapphire anvil cells. However, the limited sample amount in the opposed anvil cells is the major inconvenience for magnetization measurement in the SQUID magnetometer. To employ this type of high pressure cell in magnetic measurement, efforts is required on minimized the magnetic background of the cells as much as possible. Opposed anvil cells had not been used in SQUID magnetometer until the beginning of 21st century. This section presents the progress of opposed anvil cell for MPMS in the past 10 years.

Mito *et al.* [24] developed a first miniature diamond anvil cell (mDAC) for the MPMS in 2001. As shown in Fig. 12, the cell was made from BeCu alloy with tilt adjustments of the anvil. Pressure in this cell was calibrated by Pb and ruby fluorescence. This cell had been used perform a high pressure research on *f*-electron ferromagnetic compound $GdZn_2$ up to 4.9 GPa at the for 20000 G magnetic field. The sensitivity of this cell is around 10^{-6} emu.

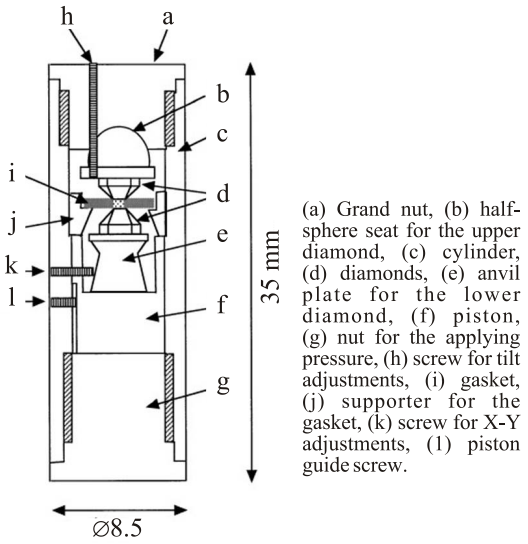

Fig. 12. Schematic drawing of the mDac. Figure reprint with permission [24].

Kobayashi *et al.* [25] developed a ZrO_2 (zirconia) opposed anvil cell for SQUID magnetometer in 2007 (Fig. 13). As shown in Fig. 13, the cell seems like a combination design of piston-cylinder cell and diamond anvil cell. The cell body was machined from BeCu alloy. Zirconia anvils were used in the cell because of its negligible magnetization. The thick gasket was made of Ni–Cr–Al. The high strength gasket enables the cell to contain greater initial sample volume with 1 mm in diameter and 1 mm in thickness, the sample space reaches 0.3 mm^3 which compensated the stronger background signal from the Ni–Cr–Al

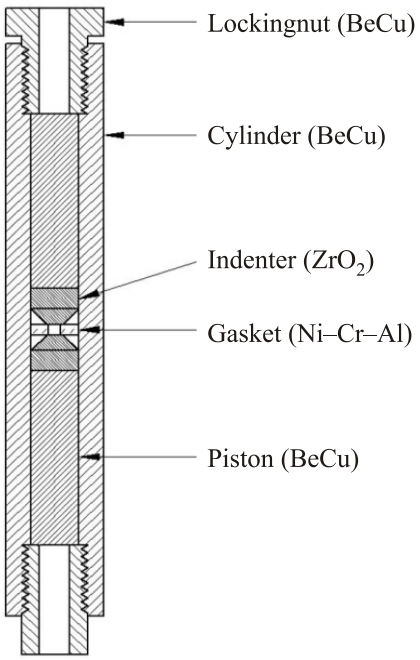

Fig. 13. Cross-sectional view of the Kobayashi's cell. Figure from Kobayashi *et al.* [25] (redrawn, not to scale).

gasket. As background signal from the gasket cannot be overlooked, the background correction of the measurement is necessary for this cell. The magnetization of the Ni–Cr–Al alloy was found depends on the aging temperature and time. 700 °C×2 h was recommended the optimal aging condition because this heat treatment provides the alloy with a small, linear magnetization which is preferable for the background subtraction. Because of the anvil is not transparent, optical access it not available for Ruby fluorescence. Therefore, pressure is only measured by superconducting transition of the manometer inside the sample. This cell had been used to gather high-pressure magnetization measurement data of UIr sample up to 4 GPa.

A break through DAC design was proposed by Alireza and Lozarich [26] on 2009 (see Fig. 14). This DAC can be considered as a modified version from the previous design. Instead of ceramic anvil, diamond anvils were used. The DAC was made from high purity CuTi alloy which has ultralow magnetic susceptibility. Pressure is generated by tightening the screw so the hollow pistons push the anvils toward each other to compress the sample in the gasket. The hollow piston provides an optical access for pressure measurement by ruby fluorescence. Alignment mechanism is highly depends on the machine quality of the cell and the anvils surface. The cell material around the sample is removed to further reduce the magnetic background signal from the cell. Apart from that, the cell body was electro polished and kept free as possible of magnetic containment. As a result, the sensitivity of this cell reach 10^{-7} emu in the experiment. The cell is capable to detect the magnetic features of phase transitions in the weakly magnetic samples based on the extremely low magnetic background.

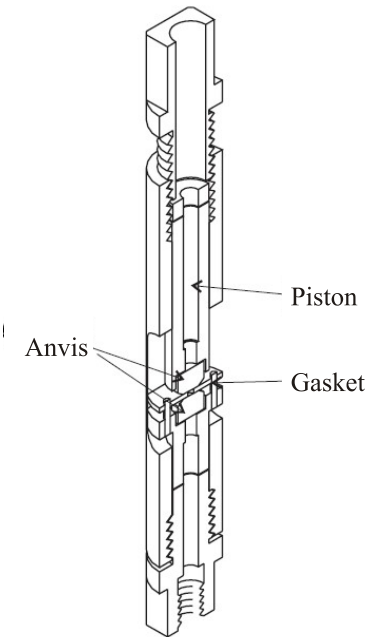

Fig. 14. Schematic drawing of the diamond anvil cell designed for MPMS. The cell is 8.4 mm in diameter and 64 mm in length. Figures from Alireza and Lozarich [26].

The ferromagnetic transition of $Cu_2Ru_2O_4$ and CoS_2 were seen clearly at high pressure even without background subtraction. In addition, antiferromagnetic transition of the $CePdGa_6$ material was detected at 4.5 GPa with the background subtraction and a pair of diamonds with larger culet diameter of 0.9 mm were used to increase sample volume. In the experimental test, the cell is capable to achieve above 14.2 GPa at room temperature with sample size of ~ 200×180×60 μm and 800 μm culet diamond.

Turnbuckle principle was first introduced in DAC design by Tozer and co-workers [27]. Turnbuckle device is widely used for bracing or losing the guy wires or cables in structural engineering, in which force can be created and maintained by rotating the body of the device while restriction the counter threaded end-nuts to translational movement. In 2010, an extremely small turnbuckle magnetic DAC (TM-DAC) for MPMS was developed by Giriat *et al.* [28]. Based on turnbuckle design, the cell is small and compact. As shown in Fig. 15, the cell 7 mm long and 7 mm in diameter and weight only 1.5 g. The cell is made of BeCu alloy and only consisting of a counter-threaded cylindrical body and two anvil supports which are identical but with external threads cut in opposite direction. The load on the diamond anvils and the sample between them is generated using a hydraulic press. The load is then locked by rotating the buckle cell body with respect to the anvil supports. No particular holder is needed for the cell as it can be loaded into a standard plastic straw holder (as shown in Fig. 15(b)). It is capable of achieving pressure in excess of 10 GPa while

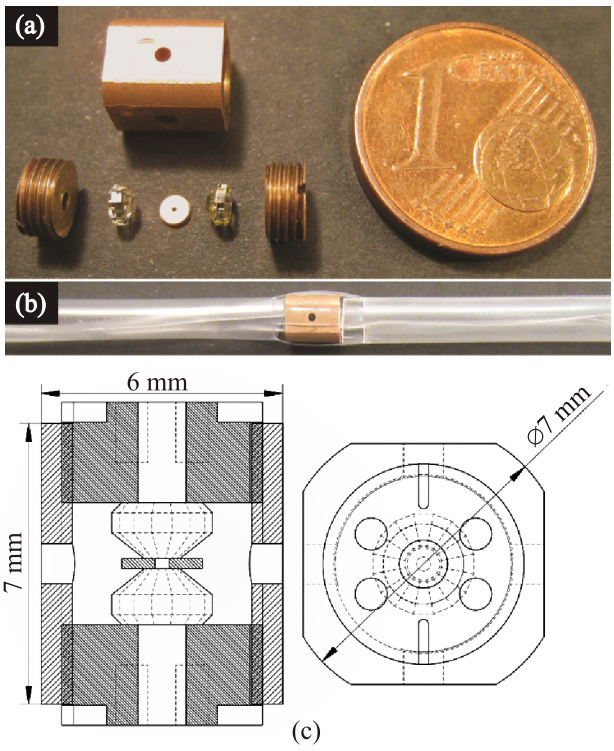

Fig. 15. (a) Parts of the TM-DAC. (b) The assemble TM-DAC in the standard plastic straw holder of MPMS. (c) Drawings of the cell with key dimensions. Figures from by Giriat *et al.* [28].

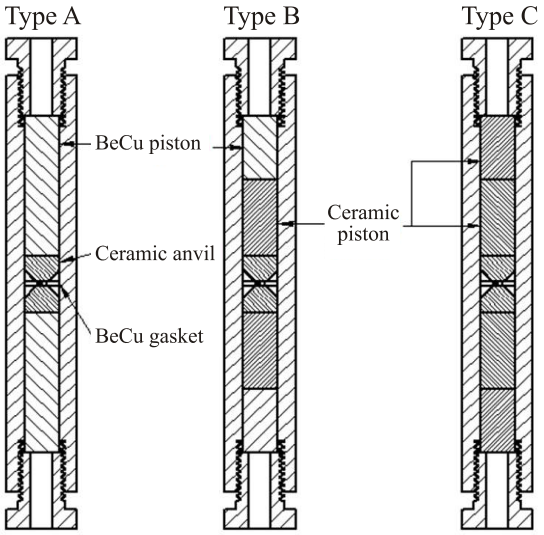

Fig. 16. Cross-sectional views of the miniature ceramic high pressure cells [29–31] (redraw, not to scale).

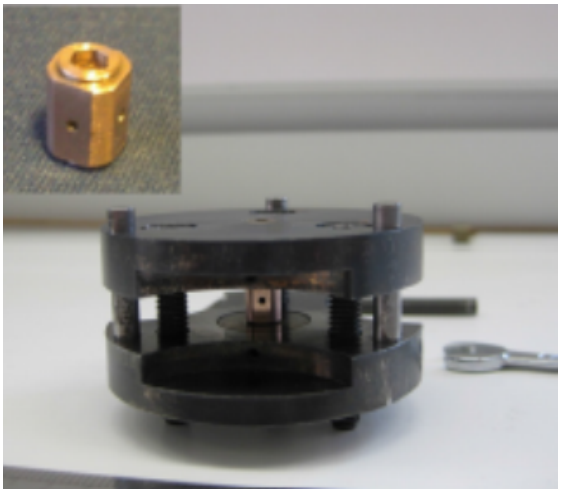

Fig. 17. The TM-^{3}He-DAC installed into the clamp for applying load (the insert shows the cell only).

allowing measurements to be performed with the maximum sensitivity (10^{-8} emu) due to the tiny size of the cell and the symmetric layout. The cell had been successful used to perform high-pressure magnetic study on $Mn_3[Cr(CN)_6]_2{\cdot}H_2O$ Prussian blue analog up to 10.3 GPa.

During 2011 and 2013, several cells called miniature ceramic anvil high pressure cell (mCAC) were developed by Tateiwa and co-workers [29–31]. As shown in Fig. 16, these cells are based on the previous cell reported by Kobayashi *et al.* [25] with several improvements. The unique feature of this cell is that the anvil was made of nonmagnetic composite ceramic (FCY20A) [32]. This material is a mixture of Y_2O_3-partially stabilized zirconia (ZrO_2) and alumina (Al_2O_3) synthesized under high temperature and high pressure. The magnetization of this newly develop ceramic is comparable to the conventional zirconia but with 2 times higher fracture toughness (6.5 MPa·m$^{1/2}$). The excellent property of this material allows the cell can be machined without an anvils alignment mechanism. The latest version type C is shown in the Fig. 16, the BeCu piston was gradually replaced by the ceramic piston to further reduced the magnetic background from the cell. BeCu gasket was used for lower magnetic background in comparison to Kobayashi's cell [25]. The main advantage of such cells is the cost effectiveness. The cost of the ceramic anvil was claimed 10 times lower than diamond anvil but with the same pressure performance. Maximum pressure was reported up to 13 GPa with 0.5 mm culet anvils and a rhenium gasket. The sample volume can be increased with cupped ceramic anvils (1 mm culet) and pressurized up to 5 GPa.

At last in this section, we present our recent progress in developing turnbuckle diamond anvil cells for magnetization measurement based on previous design reported by Giriat *et al.* [28]. The detailed information of these two turnbuckle magnetic cells will be published separately. Figure 17 presents a turnbuckle diamond anvil cell called TM-^{3}He-DAC as it is designed to work in the ^{3}He insert of the SQUID magnetometer. This cell enables the measurement of magnetic susceptibility at high pressure and at extremely low temperatures (down to 0.05 K). As the sample chamber of the ^{3}He insert from IQUANTUM [33] is limited (6.4 mm in diameter), we optimized the cell body to 6 mm in diameter and 7 mm long which is the smallest DAC so far. CuTi alloy is used to fabricate the cell to reducing the magnetic background and a specially made clamp is designed to apply load on the cell by screw. Therefore, hydraulic press in no longer needed in the cell. In a couple of pressurization tests, the cell was capable to achieved 7.4 GPa.

We had also developed a plastic version of turnbuckle DAC for used in the SQUID magnetometer to enable high pressure studies involving the ac susceptibility techniques (Fig. 18) in the commercial SQUID magnetometer. Conventionally, the high-pressure study in SQUID magneto-

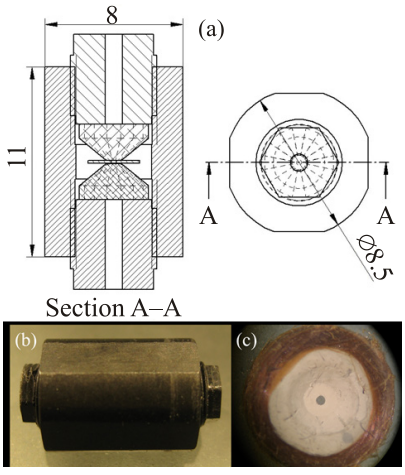

Fig. 18. (a) Drawing of the PTM-DAC with key dimensions. (b) The picture of PTM-DAC. (c) Nonmetallic gasket (unpublished).

meter has been primarily limited to dc measurements, as all the existing cells for SQUID magnetometer were made of nonmagnetic alloy which are not usable in ac measurements. The main reason is that the alternative field is applied on the sample and the cell in ac measurement, which would create eddy currents on the metallic cell. The signal from sample would be screened and the magnetization change from the sample would be unable to detect. To address this issue, we succeed in building a turnbuckle diamond anvil cell totally from nonmetallic material. The cell is made of 90HMF40 which is a carbon fiber-reinforced PEEK from Victrex [34]. Diamond and aluminum oxide powder was initially blended with epoxy. This mixture is form to an indented gasket which is then reinforced by Zylon wires. The cell had been test extensively and capable to routinely achieve 5 GPa sample pressure without failure on the cell. We can clearly read the magnetic signal from test sample Dy_2O_3 even at the highest accessible frequencies (1500 Hz) in the SQUID magnetometer.

7. High pressure cells with built-in coils for ac susceptibility measurement

Apart from using the commercial SQUID magnetometer, there had been several high-pressure magnetic measurements performing in the high pressure cells with custom-built magnetic measurement systems. This type of cells attracted increased interest to be used in magnetic study of the pressure-induced characterization of high-T_c superconductors. ac magnetic susceptibility technique (inductive method) is used in this type of cell by employing the micro and complex coils system to apply magnetic fields and pick up the magnetic signal from the stationary and pressurized sample.

In 1991, Liebenberg *et al.* [35] reported an ac susceptibility DAC (as shown in Fig. 19) used in study the pressure dependence of the superconducting transition temperature (or critical temperature) T_c in single crystal $Tl_2Ba_2CaCu_2O_8$ under nearly hydrostatic pressure up to 6 GPa. In this system, the diamond anvil cell is wound by the primary and secondary coils as shown in Fig. 20(a). BeCu gasket is used in the cell with 3.2 mm diameter and 0.56 mm thickness. The initial diameter of the sample hole is around 650 μm. Each diamond has a girdle diameter of about 4.3 mm and with 1 mm culet. The DAC is placed in a cryostat for cooling. Temperature is measured by the thermodiode attached around the diamond. The top anvil is back by a piston for applying load, bottom anvil is stationary, and the pressure is clamped at room temperature, and then placed in the sample chamber of the cryostat. The sample chamber is equipped with an optical window which allows pressure can be precisely measured by ruby fluorescence method near the critical temperature T_c. The critical temperature is determined from measurements of the ac susceptibility $\chi(T) = \chi'(T) + i\chi''(T)$ as function of temperature, where $\chi'(T)$ and $\chi''(T)$ are the real and imaginary parts of the ac susceptibility, respectively. The primary coil with 50 turns and secondary coil with 250 are wound around the anvils to match the contour of the diamonds. These coils are connected to a Hartshorn ac susceptibility bridge. A sinusoidal field of approximately 2 G at 2 kHz is produced on the sample by the primary coil. The alternating field induces an alternative voltage in the secondary coil with the same frequency, which is measured with a lock-in amplifier. The phase of the lock-in amplifier is set to separate the real and imaginary parts of the ac susceptibility. The critical temperature of the single crystal $Tl_2Ba_2CaCu_2O_8$ was found increasing nonlinearly with increasing pressure. This system was further employed in $T_c(P)$ studies of single crystals $Tl_2Ba_2Ca_2Cu_3O_{10-\delta}$ [36] and $NdBa_2Cu_3O_{7-\delta}$ [37].

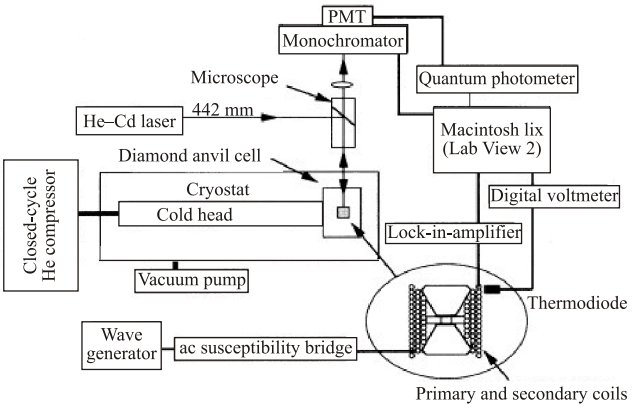

Fig. 19. Schematic diagram of the experimental setup [35–37]. The real and imaginary parts of the ac susceptibility can be measured as a function of temperature. The vacuum chamber has an optical window, so that the pressure applied to the sample at room temperature can be measured at any temperature.

The high-T_c polycrystalline compound $HgBa_2CuO_{4+\delta}$ was found to be superconducting around 94 K in 1993 [38]. As the magnetic susceptibility of this sample is relative weaker than previous high-T_c single crystal which the earlier DAC system [35] was not sensitive enough for the $T_c(P)$ study. Hence, Klehe *et al.* [39] used helium gas cell

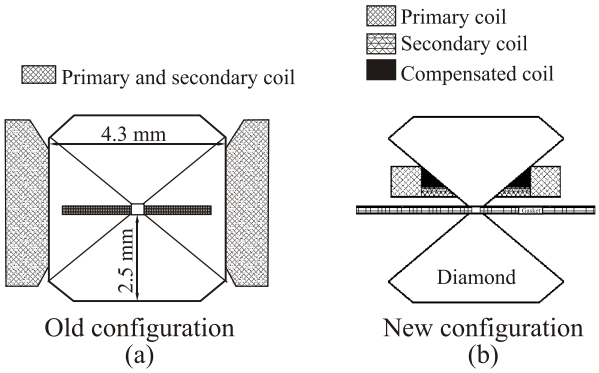

Fig. 20. The geometrical configuration of (a) the old DAC system [35–37], (b) the improved DAC system [40].

with large sample volume to perform a high-pressure magnetic measurement on this sample up to 1 GPa. In order to measure the ac susceptibility of this sample at higher pressure, Kim *et al.* [40] improved the sensitivity of the earlier DAC system [35] by modifying the geometrical configuration of the coils (Fig. 20(b)) and related circuits. The coils are wound on one diamond only in the new system. The wire diameter for the coils is 0.025 mm allowing 1600 turns/mm^2 cross section. The secondary and compensating coils have 67 and 71 turns, respectively. The number of turns is distribute in such a way that the calculate mutual inductance of each coil is nearly equal, making the total mutual inductance of two coil nearly zero. An improved bridge circuit is used in the new system to incorporate the compensating coil. In this configuration, the secondary coil (pick-up coil) is much closer to the sample, which increases the filling factor and sensitivity. The radius of the secondary coils reduces to 1 mm from 5 mm in the old configuration. A thermal radiation shield is used to cover the DAC to improve the thermometry of the system. The $T_c(P)$ of $HgBa_2CuO_{4+\delta}$ polycrystalline was measured up to 4 GPa in the improved DAC system.

A similar ac magnetic measurement system was reported by Gilder *et al.* [41] for the high-pressure magnetic measurement on the magnetite. The schematic diagram of the system is shown in Fig. 21. The system employed two unequal pick-up coils of 351 and 195 turns with diameters of 3 and 5.5 mm, which were wound in opposition around the diamond (370 μm culet) resulting in a virtually null magnetic surface. Around these was an inducing coil, mounted in null mutual inductance, which produced a peak ac field of $2\cdot10^{-4}$ T over the sample region. The coils system is housing in BeCu membrane DAC [42] which enable pressure is remotely controlled and the ac susceptibility is measured as a function of applied field.

The investigation of high pressure superconductivity by ac susceptibility technique is limited by the sample volume. Measuring the absolute ac magnetic susceptibility with ultrahigh pressure in DAC (above 50 GPa) was virtually impossible due to the very small sample in this pressure range (usually < 75 μm). However, probing the superconductivity temperature at ultrahigh pressure by using this technique is still possible as shown by Timofeev *et al.* [43]. The major difficulty in this type of study is to obtaining good coupling between the sample and sensing coil. As a result, measurement sensitivity and poor signal-to background rations need to be solved. Timofeev *et al*. [43] developed a system with modulation inductive method and resonant circuits for magnetic of superconductivity in DAC by magnetic susceptibility. As shown in Fig. 22, the complex coils system is wound around the DAC to probe the superconductivity by detection of changes in magnetic susceptibility during transition of the sample to superconducting state. The sample is located in the hole in the gasket; its location coincides with the central part of the signal coil. The ac high-frequency magnetic field at the signal coil and the sample position is created by the exciting coil fed from the high-frequency generator. The alternating magnetic field excites electromotive force in the signal coil. When transition occurs, the magnetic flux passing through the sample is expelled due to the ideal diamagnetism of the sample in the superconducting state. As a result, the magnetic flux passing through the signal coil decrease accompany with the electromotive force excited in the signal coil. Theoretically, the transition of superconducting state in the sample can be observed by measuring the electromotive force change in the signal coil. However, in the diamond anvil cell, the sample is extremely tiny if compared to the signal coil. The electromotive force from the sample is always much less than the background electromotive force originating in the signal coils. For example, the signal form the superconducting sample with a size about 100 μm does not exceed 100 nV. In comparison, the background achieves IV form the signal coil (4 mm in diameter with 300 turns under ac magnetic field with frequency 10 kHz and amplitude 0.5 Oe). An identical compensating coil (same number of turns, size, and geometry) connected in opposition to the signal coil is used to com-

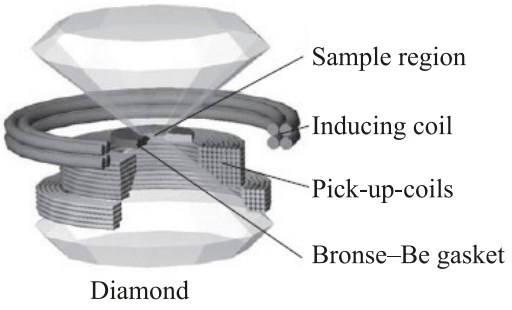

Fig. 21. The geometrical configuration of the ac susceptibility system [41]. Figure reprint with permission [41].

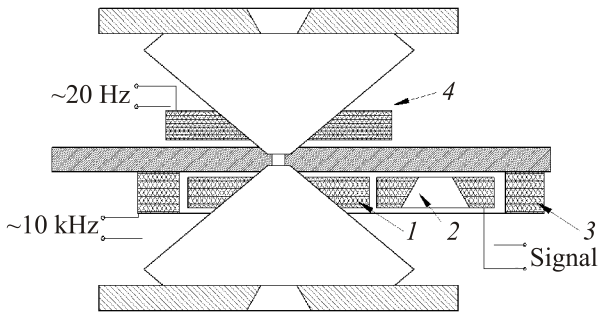

Fig. 22. Diamond anvils and coils system reported by Timofeev *et al.* [43], (*1*) signal coil, (*2*) compensating coil, (*3*) high-frequency exciting coil, (*4*) low-frequency modulating coil.

pensate the background electromotive force with a factor of 100–500. A further background reduction is needed because the system of coils is surrounded by metallic parts of the high pressure cell. The high-frequency magnetic field induced eddy currents flow through the metallic parts which distorts the magnetic flux between the signal coils and compensating coils.

In this system, another three sensitivity improvement methods are used. First, an integrated compensating block is producing an electromotive force with adjustable amplitude and phase, which is applied opposite to the background this allows the magnitude of the background signal reduced to 0.1 μV. Secondly, an additional modulating low-frequency magnetic field applied by modulating coils (as shown in Fig. 22) further suppresses the background and extracts the signal related to the superconducting transition in the sample. Last one, the application of resonant circuits with voltage increasing transformers, allowing an increase in the working frequency, with above measures, the improved system is able to detect superconductivity in tiny sample as small as 10 μm. The resonant circuit was used to obtain the superconductivity data of sulfur samples at 230 GPa.

In 2002, Jackson *et al.* [44] reported a new approach to high-pressure ac magnetic susceptibility experiments that involve specially fabricated diamond anvils with diamond encapsulated sensing microcoils, which are located just 10–20 μm from the sample. As shown in Fig. 23 (a) and (b), the magnetic sensing coil was successfully encapsulated in the diamond anvil based on the integration of three-dimensional laser pantograph, two-dimensional projection lithography [45] and epitaxial diamond chemical vapor deposition (CVD) [46]. As the 5 μm line-width microcoil is so close to the high pressure sample, the filling factor and signal-to-background ratios are improved dramatically. In this system, compensation coil or compensation circuit is no longer needed. Figure 23(c) shows the schematic drawing of the cell, the top anvil is the designer diamond with embedded sensing coil, and the bottom anvil is the normal diamond anvil wound with 55-turns excitation coil. The frequency of the driven fields in excitation coil was found optimal between 100 Hz to 10 kHz. The sensitivity of this system was shown in measuring gadolinium sample, a tiny Gd chip with a diameter 75 μm and 50 μm thickness was studied in this system, the magnetic susceptibility data as a function of temperature was collect clearly in the experiment.

An unique indenter-type high pressure cell for magnetic measurements was reported in 2007 by Kobayashi *et al.* [25]. The cell is able to perform both NMR and ac susceptibility measurement on sample. A cross-sectional drawing is shown in Fig. 24(a), the cell is composed of four parts: an indenter, a NiCrAl hole piece, an cell body and a locknut made from BeCu. The initial size of the sample hole is 1.6 mm in diameter and 1.4 mm in depth, which provides

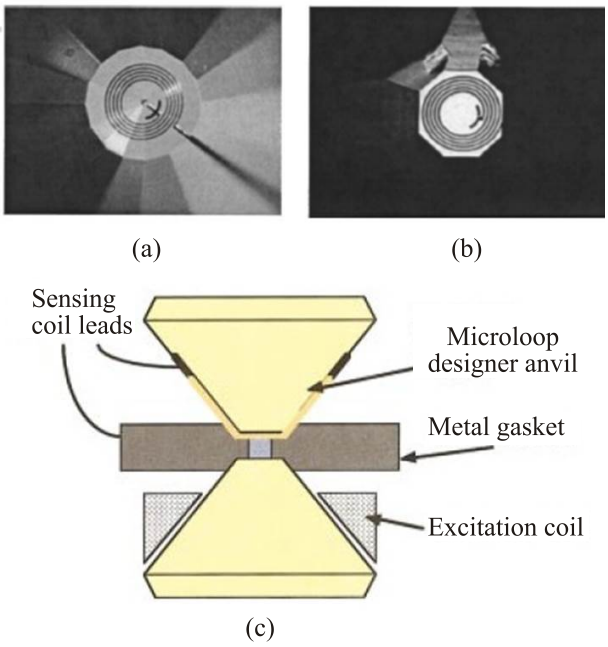

Fig. 23. Five turns multiloop in the designer anvil (a) after lithographic fabrication of the microcoils, (b) view with transmitted light. (c) The schematic view of the cell. Figures from Jackson *et al.* [44].

approximately 0.9 mm^3 sample space. The cone shaped indenter is made of nonmagnetic tungsten carbide (NMWC). The diameter of the indenter is 10 mm and the angle of the cone is 90°. The culet of the indenter is 1.4 mm which is slightly smaller the sample hole. The bore of the cell body

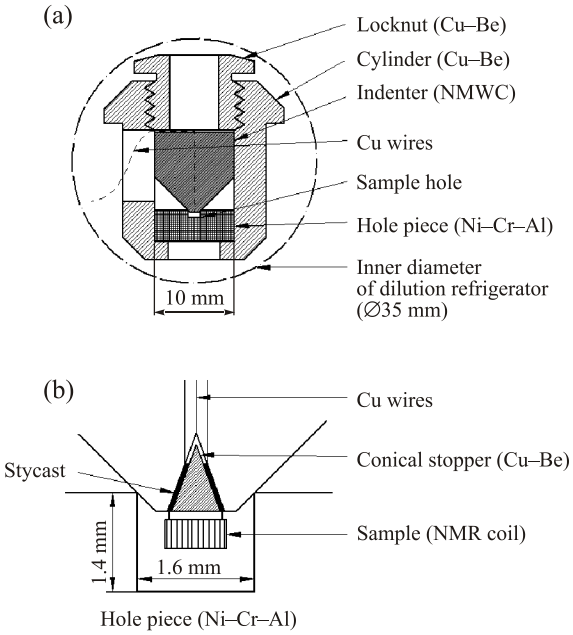

Fig. 24. (a) Cross-sectional view of the indenter cell, (b) arrangement for electrical resistance and NMR measurements in the indenter cell, in ac susceptibility measurement, the coils is replaced to ac susceptibility coils which primary coil wounds directly onto the secondary coil. Figure from Kobayashi *et al.* [25].

is used as a guide when the indenter is sliding inside. The working mechanism of this cell is similar to conventional piston-cylinder cell. A loading force is applied by using a hydraulic press. A columnar pusher inserted in the hole of the locknut to transmit the load on the indenter. The sample pressure is generated when the indenter deforms the contact edge around the sample hole. Then the pressure is clamped by rotating the locknut. As shown in Fig. 24(b), a sample and Pb manometer were placed on the base of the conical stopper inside the coils for measurement and pressure calibration in low temperature. This miniature coil is prepared in the sample space to gain a large filling factor for the sample. By this setup, the Meissener effect and the ferromagnetic transition of the pressure-induced superconductors UIr and $CeNiGe_3$ were successfully observed up to 4.5 GPa.

Outline and conclusion

We have reviewed two categories high pressure cell for the most widely used commercial SQUID magnetometer and some high pressure cells with build-in coils for magnetic measurements. High-pressure instrumentation for the SQUID magnetometer is much more convenient and for researchers as system setup in the built-in coils cell is complicated and inconvenient.

1. A. Galkin, E.A. Zavadskii, V.M. Smirnov, and V.I. Valkov, *JETP Lett*. **20**, 111 (1974).
2. *http://www.qdusa.com*
3. *http://www.ngkberylco.co.uk/*
4. K. Kamishima, M. Hagiwara, and H. Yoshida, *Rev. Sci. Instrum*. **72**, 1472 (2001).
5. D. Wohlleben and M. Maple, *Rev. Sci. Instrum*. **42**, 1573 (1971).
6. R.P. Guertin and S. Foner, *Rev. Sci. Instrum.* **45**, 863 (1974).
7. K. Koyama, S. Hane, K. Kamishima, and T. Goto, *Rev. Sci. Instrum*. **69**, 3009 (1998).
8. M. Eremets, *High Pressure Experimental Methods*, Oxford University Press (1996).
9. Y. Uwatoko, S. Todo, K. Ueda, A. Uchida, M. Kosaka, N. Mori, and T. Matsumoto, *J. Phys.: Condens. Matter* **14**, 11291 (2002).
10. I.R. Walker, *Rev. Sci. Instrum*. **70**, 3402 (1999).
11. D.E. Graf, R.L. Stillwell, K.M. Purcell, and S.W. Tozer, *High Press. Res*. **31**, 533 (2011).
12. A. Eiling and J.S. Schilling, *J. Phys.: F. Met. Phys*. **11**, 623 (1981).
13. J.D. Barnett, S. Block, and G.J. Piermarini, *Rev. Sci. Instrum*. **44**, 1 (1973).
14. J. Kamarád, Z. Machátova, and Z. Arnold, *Rev. Sci. Instrum*. **75**, 5022 (2004).
15. J. Sanchez-Benitez, S. Tancharakon, M. Hutchison, and K.V. Kamenev, *J. Phys.: Conf. Ser.* **121**, 122001 (2008).
16. S. Reich and T. Godin, *Meas. Sci. Technol*. **7**, 1079 (1996).
17. J. Diederichs, A. Gangopadhyay, and J. Schilling, *Phys. Rev. B* **54**, R9662 (1996).
18. EasyLab. easyLab Mcell 10 (2004).
19. I. Umehara, F. Tomioka, A. Tsuboi, T. Ono, M. Hedo, and Y. Uwatoko, *J. Magn. Magn. Mater*. **272–276**, 2301 (2004).
20. Y. Uwatoko, T. Fujiwara, M. Hedo, F. Tomioka, and I. Umehara, *J. Phys.: Condens. Matter* **17**, S1011 (2005).
21. K.V. Kamenev, S. Tancharakorn, N. Robertson, and A. Harrison, *Rev. Sci. Instrum*. **77**, 073905 (2006).
22. J. Kamarád, M. Mihalik, V. Sechovský, and Z. Arnold, *High Press. Res.* **28**, 633 (2008).
23. S. Titos-Padilla, J.M. Herrera, X.-W. Chen, and J.J. Delgado, *Angew. Chem. Int. Ed. Engl*. **50**, 3290 (2011).
24. M. Mito, M. Hitaka, T. Kawae, K. Takeda, T. Kitai, and N. Toyoshima, *Jpn. J. Appl. Phys*. **40**, 6641 (2001).
25. T.C. Kobayashi, H. Hidaka, H. Kotegawa, K. Fujiwara, and M.I. Eremets, *Rev. Sci. Instrum*. **78**, 023909 (2007).
26. P.L. Alireza and G.G. Lonzarich, *Rev. Sci. Instrum*. **80**, 023906 (2009).
27. C. Martin, C.C. Agosta, S.W. Tozer, H.A. Radovan, T. Kinoshota, and M. Tokumoto, *J. Low Temp. Phys*. **138**, 1025 (2005).
28. G. Giriat, W. Wang, J.P. Attfield, A.D. Huxley, and K.V. Kamenev, *Rev. Sci. Instrum*. **81**, 073905 (2010).
29. N. Tateiwa, Y. Haga, Z. Fisk, and Y. Ōnuki, *Rev. Sci. Instrum*. **82**, 053906 (2011).
30. N. Tateiwa, Y. Haga, T.D. Matsuda, and Z. Fisk, *Rev. Sci. Instrum*. **83**, 053906 (2012).
31. N. Tateiwa, Y. Haga, T.D. Matsuda, Z. Fisk, S. Ikeda, and H. Kobayashi, *Rev. Sci. Instrum*. **84**, 046105 (2013).
32. FCY 20A, *http://www.fujidie.co.jp/*
33. IQUANTUM, *http://www.iquantum.co.jp/eng/ pro.html*
34. Victrex® peek.
35. N. Moulton, S. Wolf, E. Skelton, D.H. Liebenberg, T.A. Vanderah, A.M. Hermann, and H.M. Duan, *Phys. Rev. B* **44**, 12632 (1991).
36. D. Berkley, E. Skelton, N. Moulton, M.S. Osofsky, W.T. Lechter, V.M. Browning, and D.H. Liebenberg, *Phys. Rev. B* **47**, 5524 (1993).
37. C. Kim, E. Skelton, M. Osofsky, and D. Liebenberg, *Phys. Rev. B* **48**, 6431 (1993).
38. S.N. Putilin, E.V. Antipov, O. Chmaissem, and M. Marezio, *Nature* **362**, 226 (1993).
39. A.-K. Klehe, A.K. Gangopadhyay, J. Diederichs, and J.S. Schilling, *Phys. Supercond. C* **213**, 266 (1993).
40. C.C. Kim, M.E. Reeves, M.S. Osofsky, E.F. Skelton, and D.H. Liebenberg, *Rev. Sci. Instrum*. **65**, 992 (1994).
41. S.A. Gilder, *Geophys. Res. Lett*. **29**, 1392 (2002).
42. J.C. Chervin, B. Canny, J.M. Besson, and P. Pruzan, *Rev. Sci. Instrum*. **66**, 2595 (1995).
43. Y.A. Timofeev, V.V. Struzhkin, R.J. Hemley, H. Mao, and E.A. Gregoryanz, *Rev. Sci. Instrum*. **73**, 371 (2002).
44. D.D. Jackson, C. Aracne-Ruddle, V. Malba, S.T. Weir, S.A. Catledge, and Y.K. Vohra, *Rev. Sci. Instrum*. **74**, 2467 (2003).
45. B.M. McWilliams, I.P. Herman, F. Mitilitsky, R. Hyde, and L. Wood, *Appl. Phys. Lett*. **43**, 946 (1983).
46. S.T. Weir, J. Akella, C. Aracne-Ruddle, Y.K. Vohra, and S.A. Catledge, *Appl. Phys. Lett*. **77**, 3400 (2000).